Accepted Manuscript

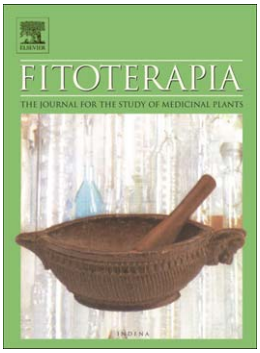

Chemo-protective and regenerative effects of diarylheptanoids from the bark of black alder (*Alnus glutinosa*) in human normal keratinocytes

Jelena Dinić, Teodora Ranelović, Tijana Stanković, Miodrag Dragoj, Aleksandra Isaković, Miroslav Novaković, Milica Pešić

PII: S0367-326X(15)30040-X
DOI: doi: 10.1016/j.fitote.2015.07.003
Reference: FITOTE 3220

To appear in: *Fitoterapia*

Received date: 28 April 2015
Revised date: 30 June 2015
Accepted date: 2 July 2015

Please cite this article as: Jelena Dinić, Teodora Ranelović, Tijana Stanković, Miodrag Dragoj, Aleksandra Isaković, Miroslav Novaković, Milica Pešić, Chemo-protective and regenerative effects of diarylheptanoids from the bark of black alder (*Alnus glutinosa*) in human normal keratinocytes, *Fitoterapia* (2015), doi: 10.1016/j.fitote.2015.07.003

Chemo-protective and regenerative effects of diarylheptanoids from the bark of black alder (*Alnus glutinosa*) in human normal keratinocytes

Jelena Dinić[a*], Teodora Ranđelović[a], Tijana Stanković[a], Miodrag Dragoj[a], Aleksandra Isaković[b], Miroslav Novaković[c], Milica Pešić[a*]

[a]*Institute for Biological Research, Department of Neurobiology, University of Belgrade, Bulevar Despota Stefana 142, Belgrade, Serbia*

[b]*Faculty of Medicine, University of Belgrade, Doktora Subotića 8, Belgrade, Serbia*

[c]*Institute for Chemistry, Technology and Metallurgy, University of Belgrade, Studentski trg 12-16, Belgrade, Serbia*

***Corresponding authors**

dr Jelena Dinić

dr Milica Pešić

Institute for Biological Research, Department of Neurobiology, University of Belgrade, Despota Stefana Boulevard 142, Belgrade, Serbia

Phone: +381 11 20 78 406

Fax: +381 11 27 61 433

E-mail: jelena.dinic@ibiss.bg.ac.rs (J. Dinić); camala@ibiss.bg.ac.rs (M. Pešić)

Abstract

Medicinal plants are recognized from ancient times as a source of diverse therapeutic agents and many of them are used as dietary supplements. Comprehensive approaches are needed that would identify bioactive components with evident activity against specific indications and provide a better link between science (ethno-botany, chemistry, biology and pharmacology) and market. Recently, the bark of black alder (*Alnus glutinosa*) appeared at market in the form of food supplement for treatment of different skin conditions. This study aimed to evaluate protective effects of two diarylheptanoids isolated from the bark of black alder: platyphylloside - 5(*S*)-1,7-di(4-hydroxyphenyl)-3-heptanone-5-O-*β*-D-glucopyranoside (**1**) and its newly discovered analog 5(*S*)-1,7-di(4-hydroxyphenyl)-5-O-*β*-D-[6-(*E*-*p*-coumaroylglucopyranosyl)]heptane-3-one (**2**) towards doxorubicin damaging activity. To that end, we employed HaCaT cells, non-cancerous human keratinocytes commonly used for skin regenerative studies. Diarylheptanoids significantly antagonized the effects of doxorubicin by lowering the sensitivity of HaCaT cells to this drug. Compound **2** prevented doxorubicin-induced cell death by activating autophagy. Both **1** and **2** protected HaCaT cells against doxorubicin-induced DNA damage. They significantly promoted migration and affected F-actin distribution. These results indicate that chemo-protective effects of diarylheptanoids may occur at multiple subcellular levels. Therefore, diarylheptanoids **1** and **2** could be considered as protective agents for non-cancerous dividing cells during chemotherapy.

Keywords

diarylheptanoid; curcumin; doxorubicin; DNA damage; cell motility; chemoprotection

Introduction

For approximately 85% of the world's population, plant materials are a primary source of health care [1]. Natural products drug discovery could be beneficial for the major lethal diseases such as cancer, as there are still no satisfactory drug treatments. Besides food, plant products and extracts are widely used as spices, cosmetics and pharmaceutical agents [2]. Our attention was drawn by the plants from the *Alnus* genus well known for their traditional medicinal values. These plants have been used for the treatment of various diseases including cancer. Particularly, we were interested in the bark of black alder (*Alnus glutinosa*) because of its beneficial effects on different skin problems [3].

Many products from the bark of black alder currently on the market are used as food supplements to treat different chronic dermatological conditions. However, they are still not approved by the Food and Drug Administration (FDA) and extensive studies of chemically defined bioactive components present in such supplements are needed.

While other *Alnus* species have been widely studied, there are few reports describing the secondary metabolites found in the seeds and bark of *Alnus glutinosa* [4-7].

Diarylheptanoids are common phenolic compounds consisting of two aromatic rings connected by a heptane chain abundant in the *Alnus* species [8-9], but also found in *Zingiber*, *Curcuma*, *Alpinia* and *Betula* genera. Curcumin is the most investigated diarylheptanoid isolated from *Curcuma longa* (Zingiberaceae) with a wide range of biological activities [10-14]. Diarylheptanoids have been shown to exhibit antioxidative

[15-16], anti-inflammatory [17], antiviral [18], cytotoxic [19-21], or anti-cancer effects [22]. Recently, we reported that diarylheptanoids from the bark of *Alnus glutinosa* possess chemo-protective activity in human lymphocytes DNA [6]. Moreover, they were able to protect the integrity of mitochondria and increase antioxidant capacity of normal cells [23].

Herein we further investigated dermo-protective actions of diarylheptanoids from the bark of black alder using human normal keratinocytes. The effects were assessed on a subcellular level, including the effects on DNA damage, autophagy and cell motility.

Materials and methods

Drugs

Doxorubicin (DOX) solution was obtained from EBEWE Arzneimittel GmbH, Vienna, Austria. Curcumin (CUR) was purchased from Sigma-Aldrich Chemie GmbH, Germany and diluted in absolute ethanol. AZD2014 was a kind gift from SelleckChem, Houston, TX, USA. Diarylheptanoids **1** and **2** were isolated from *A. glutinosa* bark as described previously [6]. The yield of compounds **1** and **2** are 0.33% and 0.033%, respectively (calculated on extract) or 0.08% and 0.008% respectively (calculated on dry plant material) [6].

Chemicals

RPMI 1640 medium, DMEM medium, penicillin–streptomycin solution, antibiotic–antimycotic solution, L-glutamine and trypsin/EDTA were purchased from

PAA, Vienna, Austria. Fetal bovine serum (FBS), dimethyl sulfoxide (DMSO) and Hoechst 33342 were obtained from Sigma–Aldrich Chemie GmbH, Germany. Bovine serum albumin was from Serva, Heidelberg, Germany, and Triton™ X-100 from Merck KGaA, Darmstadt, Germany. Propidium Iodide (PI) and Annexin-V-FITC (AV) were purchased from Abcam, Cambridge, UK. ActinRed™ 555 was obtained from Molecular Probes®, Invitrogen Life Technologies, CA, USA. Anti-LC3B antibody was from Abcam (Cambridge, UK). Phospho-histone H2A.X antibody was from Cell Signaling Technology Inc. (Danvers, Massachusetts, USA) and secondary antibody Alexa Fluor 488 goat anti-Rabbit IgG(H+L) was purchased from Invitrogen Life Technologies.

Cell culture

HaCaT cell line (human normal keratinocytes obtained from CLS - Cell Lines Service, Eppelheim, Germany) was a generous gift from Prof. Andra Jorg, Division of Biophysics, Research Center Borstel, Leibniz-Center for Medicine and Biosciences, Borstel, Germany. 518A2 melanoma cell line was obtained from the American Type Culture Collection, Rockville, MD, USA. Both cell lines were cultured in DMEM supplemented with 10% FBS, 4 g/L glucose, L-glutamine (2 mM) and 5000 U/ml penicilin, 5 mg/mL streptomycin solution.

Cytotoxicity by MTT assay

Cell viability was assessed by MTT assay (MTT, Sigma, St. Louis, MO). Briefly, cells were seeded in 96-well microplates and treated with increasing concentrations of **1**, **2**, CUR and DOX for 72 h. For combination treatments, cells were pretreated with 5 μM

of **1**, **2** or CUR at 37 °C for 6 h and subsequently treated with increasing concentrations of DOX. The absorbance of formazan dye was measured at 540 nm using an automatic microplate reader (LKB 5060-006 Micro Plate Reader, Vienna, Austria).

Growth inhibition (I) was determined according to the following equitation:

$$I = (1 - \frac{A_{treated}}{A_{untreated}}) \times 100$$

where A is absorbance.

IC_{50} value was defined as a concentration of each drug that inhibited cell growth by 50%. IC_{50} was calculated by linear regression analysis using Excel software.

Median effect analysis

The nature of the interaction between different drugs was analyzed using CalcuSyn software (Biosoft, Cambridge, UK) that uses the combination index (CI) method [24], based on the multiple drug effect equation. Values of log10 (CI) < 0 point to a pronounced additive effect or synergism, log10 (CI) = 0 indicates an additive effect, and log10 (CI) > 0 points to an antagonistic effect.

Cell death detection

The percentages of apoptotic, necrotic and viable cells were determined by Annexin-V-FITC (AV) and propidium iodide (PI) labeling. HaCaT cells were incubated overnight in 6-well plates and subjected to single treatments with 5 μM **1**, **2** and CUR. In combined treatments, cells were pretreated with 5 μM **1**, **2** or CUR at 37 °C for 6 h and subsequently treated with 40 nM DOX. After 72 h, the attached and floating cells were

collected by centrifugation. AV/PI staining was performed according to manufacturer's instructions and cells were analyzed within 1 h by flow-cytometry. The fluorescence intensity (green FL1-H and red FL2-H) was measured on FACSClibur flow-cytometer (Becton Dickinson, Oxford, United Kingdom). In each sample, 10,000 cells were recorded (gated to exclude cell debris), and the percentages of viable (AV- PI-), early apoptotic (AV+ PI-), apoptotic and necrotic (AV+ PI+), and already dead (AV- PI+) cells were analyzed by CellQuest Pro data analysis software.

Fluorescence microscopy

HaCaT cells were seeded in chamber-slides (Nunc, Naperville, IL, USA) and allowed to grow at 37°C overnight before treatment. Subsequently, the cells were treated with 5 μM **1** and **2** for 18 h at 37 °C. 250 nM AZD2014, which induces autophagy by inhibiting the mTOR complex, was used as a positive control. To detect autophagosomes, cells were washed in PBS, fixed in 4% paraformaldehyde, and blocked for 60 min with 2% bovine serum albumin in 0.3% Triton™ X-100 in PBS. Rabbit anti-LC3B antibody was applied at 1:1000 dilution in PBS/0.3% Triton X-100 and cells were incubated over night at 4°C. After washing in PBS, secondary antibody Alexa Fluor 488 goat anti-Rabbit IgG(H+L) was applied at 1:1000 dilution in PBS/0.3% Triton X-100 for 120 min at room temperature. Nuclei were counterstained with Hoechst 33342 for 15 min at room temperature and cells were mounted in Mowiol. HaCaT cells were examined under the Zeiss Axiovert fluorescent microscope (Carl Zeiss Foundation, Oberkochen, Germany) using AxioVision4.8 software.

To evaluate the effect of diarylheptanoids on the cytoskeleton structure, HaCaT cells were treated with 5 μM **1, 2** and CUR for 24 h at 37 °C. After treatment, cells were washed in PBS, fixed in 4% paraformaldehyde and labeled for 30 min at room temperature with ActinRed™ 555 which binds to F-actin. Nuclei were counterstained with Hoechst 33342 for 15 min at room temperature and cells were examined under the Zeiss Axiovert fluorescent microscope.

To detect DNA damage, HaCaT cells were labeled with phospho-histone H2A.X (Ser^{139}) antibody. This antibody detects endogenous levels of phosphorylated H2AX which is recruited to sites of double strand DNA breaks. Prior to immunostaining, cells were subjected to single treatments with 20 nM DOX or 5 μM **1**, **2** and CUR for 18 h at 37 °C. In combined treatments, cells were pretreated with 5 μM **1**, **2** and CUR at 37 °C for 6 h and subsequently treated with 20 nM DOX for additional 18 h. After treatment, cells were washed in PBS, fixed in 4% paraformaldehyde, and blocked for 60 min with 2% bovine serum albumin in 0.3% Triton™ X-100 in PBS. Rabbit anti-phospho-histone H2A.X antibody was applied at 1:1000 dilution in PBS/0.3% Triton X-100 and cells were incubated over night at 4°C. After washing in PBS, secondary antibody Alexa Fluor 488 goat anti-Rabbit IgG(H+L) was applied at 1:1000 dilution in PBS/0.3% Triton X-100 for 120 min at room temperature. Nuclei were counterstained with Hoechst 33342 for 15 min at room temperature and cells were mounted in Mowiol. The cells were examined under the Zeiss Axiovert fluorescent microscope.

Detection of autophagic flux by flow cytometry

The fluorescence intensity of anti-LC3B antibody coupled with secondary antibody Alexa Fluor 488 goat anti-Rabbit IgG(H+L) was used to assess autophagic flux by flow-cytometric analysis. HaCaT cells were incubated overnight in 6-well plates, and then subjected to treatments with 5 μM **1**, **2** and CUR or 250 nM AZD2014 for 18 h at 37 °C. Adherent cells were harvested by trypsinization, washed twice in PBS, fixed in 4% paraformaldehyde for 10 min at room temperature. HaCaT cells were then permeabilized by adding ice-cold 90% methanol and stored at -20 °C overnight. After washing in PBS, cells were blocked for 60 min with 0.5% bovine serum albumin in PBS. Cells were then resuspended in 100 μl of primary antibody diluted in 0.5% bovine serum albumin (1:1000) and incubated 60 min at room temperature. After washing in PBS, cells were resuspended in 100 μl of fluorochrome-conjugated secondary antibody (1:1000) and incubated for 30 min at room temperature. HaCaT cells were subsequently washed and resuspended in 500 μl of PBS. The fluorescence intensity (FL1-H channel) was measured on FACSClibur flow-cytometer (Becton Dickinson, Oxford, United Kingdom). A minimum of 10,000 events were assayed for each sample.

Detection of double strand DNA breaks by flow cytometry

The fluorescence intensity of anti-phospho-histone H2A.X antibody coupled with secondary antibody Alexa Fluor 488 goat anti-Rabbit IgG(H+L) was used to quantify double strand DNA breaks by flow-cytometric analysis. HaCaT cells were incubated overnight in 6-well plates, and then subjected to single treatments with 20 nM DOX or 5 μM **1**, **2** and CUR for 18 h at 37 °C. In combined treatments, HaCaT cells were pretreated with 5 μM **1**, **2** and CUR at 37 °C for 6 h and subsequently treated with 20 nM DOX for

additional 18 h. Adherent cells were harvested by trypsinization, washed twice in PBS, fixed in 4% paraformaldehyde for 10 min at room temperature. Anti-phospho-histone H2A.X antibody staining for flow cytometry was performed in the same manner as previously described anti-LC3B antibody staining. The fluorescence intensity (FL1-H channel) was measured on FACSClibur flow-cytometer (Becton Dickinson, Oxford, United Kingdom). A minimum of 10,000 events were assayed for each sample.

Wound healing assay

HaCaT cells were seeded in 24-well plates and grown for 24 h at 37ºC. Upon reaching confluence, a uniform wound was scratched into a monolayer of each well with a sterile plastic 200 μL micropipette tip. After wounding, tissue culture medium was replaced and cells were treated with 5 μM diarylheptanoids **1**, **2** and CUR. Wound closure was monitored by imaging cells at 2x magnification on a Leica microscope (Leica Microsystems GmbH, Wetzlar, Germany) at the moment of wounding and at 24 h post-wounding. The captured images were analyzed by ImageJ software (NIH, USA) to measure the degree of closure of the wounded area.

Statistical analysis

The differences between groups were examined by Student's t-test (Statistica 6.0 software) and one-way or two-way ANOVA test (GraphPad Prism software). Statistical significance was accepted if $p<0.05$.

Results and discussion

*Diarylheptanoids **1** and **2** antagonize the effects of DOX in human normal keratinocytes*

In this study, we were focused on dermo-protective effects of diarylheptanoids from *Alnus glutinosa*. To that end, we used human normal keratinocytes (HaCaT) as a model for our investigation. In our previous search for naturally occurring anti-cancer agents with low toxicity towards normal cells, we distinguished two diarylheptanoids with such characteristics: platyphylloside (**1**) and its recently discovered analog with *p*-coumaroyl group (**2**) (Fig. 1A) [7, 23]. Therefore, we compared the growth inhibitory effects of **1**, **2**, curcumin (CUR) and doxorubicin (DOX) in human melanoma (518A2) and HaCaT cells. The effects were analyzed after 72 h by MTT assay. The results are summarized as IC_{50} values and shown in Table 1. Although DOX was efficient in nanomolar range showing stronger anti-cancer potential, it was not selective towards melanoma cells since the IC_{50} values for DOX obtained in 518A2 and HaCaT cells were 24.5 nM and 6.7 nM, respectively. Similarly, diarylheptanoid **1** and CUR were non-selective, but in micromolar range, while compound **2** induced more prominent growth inhibition in melanoma cells with IC_{50} values 24 μM for 518A2 and 35.2 μM for HaCaT (Table 1).

Knowing that diarylheptanoids from the bark of black alder possess cyto- and nucleo-protective effects [6, 23], we wondered whether **1** and **2** may protect HaCaT cells which are significantly sensitive to DOX. In order to study the interaction of each diarylheptanoid with DOX, we applied these drugs subsequently. Namely, after 6 h pretreatment with **1** or **2**, HaCaT cells were incubated for additional 72 h with different concentrations of DOX. Diarylheptanoids **1** and **2** desensitized HaCaT cells to DOX by

increasing its IC_{50} values in combined treatments (Fig. 1B). The activity of these compounds was compared next to CUR, a well investigated diarylheptanoid with multiple therapeutic properties. We revealed that CUR was less protective against DOX in HaCaT cells. The results obtained with combinations were then analyzed by CalcuSyn software to assess the nature of the interaction between two different drugs (synergism/antagonism). All combinations with **1** or **2** and DOX demonstrated pronounced antagonistic effect. The observed antagonism was less apparent when CUR was applied (Fig. 1C).

*Diarylheptanoid **2** prevents cell death induced by DOX in human normal keratinocytes*

Next, we studied the mechanisms by which diarylheptanoids from the bark of black alder exert their DOX-antagonistic effects in HaCaT cells. Apoptosis induction is a main mechanism of action in most chemotherapeutic agents including DOX [25-27], However, cytotoxicity exhibited by DOX on normal cells is an adverse side effect during the course of chemotherapy in cancer patients.

To study the effect of compounds **1** and **2** on cell death, HaCaT cells treated with diarylheptanoids alone or in subsequent combination with DOX were subjected to Annexin-V-FITC/Propidium Iodide staining (Fig. 2A). Flow cytometry analysis revealed cell death-inducing activity of 40 nM DOX (11% of cells in apoptosis and 11% of cells in late apoptosis and necrosis). After the treatment with 5 μM of **1** the percentage of apoptotic HaCaT cells increased compared to untreated control (from 4% to 19%). Diarylheptanoid **1** combined with DOX reduced the percentage of late apoptotic and necrotic cells observed when 40 nM DOX was applied alone (Fig. 2A). Diarylheptanoid

2 did not induce cell death and completely prevented DOX effect in normal keratinocytes (Fig. 2A). By this means, both diarylheptanoids, particularly diarylheptanoid **2**, showed the potential for DOX-protective action. Quantification and statistical analysis of the results obtained by flow cytometry for each condition is shown in Fig. 2B.

*Diarylheptanoid **2** promotes autophagy in human normal keratinocytes*

In addition to apoptosis, the effect of compounds **1** and **2** on the autophagy process was also examined in HaCaT cells. Apoptosis and autophagy are not independent processes, and many stress pathways activate both autophagy and apoptosis within the same cell. Autophagy is a defense mechanism which involves degradation and recycling of intracellular components as a response to stress [28]. Depending on cell type and physiological conditions, autophagy has a dual role in cellular homeostasis, both promoting cell survival and apoptosis [29-30]. Normally, autophagy prevents the induction of apoptosis, and vice versa apoptosis-related activation of caspases inhibits the autophagic process [31].

LC3B, the ubiquitin-like protein microtubule-associated protein-1 light chain 3, is an essential mediator of autophagosome formation [32]. The key step in autophagosome biogenesis is the conversion of the unconjugated form LC3B-I to its phosphatidylethanolamine (PE)-conjugated and membrane-associated form LC3B-II [33-34]. LC3B-II is integrated in the outer autophagosome membrane until the the late stages of autophagy, when it's recycled by ATG4B, whereas LC3B-II on the inner membrane is degraded by lysosomal activity after autophagosome–lysosome fusion [32].

Autophagic vesicles labeled with anti-LC3B antibody were visualized in HaCaT cells after 18 h exposure to 5 μM CUR, **1** and **2** (Fig. 2C). The effects of investigated agents were compared next to 250 nM AZD2014, mTOR inhibitor and an autophagy inducing agent used as a positive control. Similar to AZD2014, diarylheptanoid **2** triggered the activation of the autophagy pathway and caused the formation of autophagosomes in the cytoplasm of HaCaT cells. Treatments with **1** and CUR did not lead to the appearance of autophagic vesicles (Fig. 2C). This supports our previous finding that **2**, which possess a *p*-coumaroyl group is more selective towards cancer cells and more beneficial for normal cells than its related diarylheptanoid **1** [7].

Flow cytometry is a sensitive and precise method for analyzing autophagic flux in cells as LC3B-II protein serves as a potential autophagic substrate for degradation [35-37]. Consequently, any changes in total intracellular LC3B fluorescence intensity represent autophagic activity in cells. Increased autophagic flux results in a continuous delivery of LC3B-II to autophagolysosome where this protein undergoes degradation by lysosomal enzymes. Enhanced autophagic flux is detected as a decrease in total cellular signal of fluorescently labeled LC3B. On contrary, inhibition of autophagic flux leads to accumulation of non-degraded LC3B and increases intracellular LC3B signal.

HaCaT cells were treated for 18 h with 5 μM diarylheptanoids or 250 nM AZD2014, fixed and labeled with anti-LC3B antibody (Fig. 2D). Flow cytometry analysis showed a decline in overall LC3B content in cells treated with compound **2**, similarly to AZD2014 treatment. Interestingly, compound **1** increased the cytosolic pool of LC3B but did not promote autophagosome formation, while curcumin treatment had no significant effect on LC3B levels in HaCaT cells (Fig. 2D). Quantification and

statistical analysis of flow-cytometric measurements of autophagic flux after treatment with diarylheptanoids is shown in Fig. 2E.

Since apoptosis and autophagy can be activated by common upstream signals and share molecular components that directly regulate both processes, the onset of autophagy induced by **2** might be responsible for the reduced apoptosis observed in DOX-exposed cells.

*Diarylheptanoids **1** and **2** protect human normal keratinocytes against DOX-induced DNA damage*

It was previously reported that compounds **1** and **2** exhibit *in vitro* chemo-protective effect on chromosome aberrations induced by clastogenic agent mitomycin C in peripheral human lymphocytes [6]. Studies have shown that CUR can exhibit both protective and damaging effects on human DNA [38-41]. On the other side, DOX is a DNA-intercalating agent which inhibits macromolecular biosynthesis [42]. One of its main mechanisms of action is the negative effect on the topoisomerase II progression, whose role is to relax DNA supercoils for transcription [43]. Another effect of DOX is the eviction of histones from chromatin which disturbs the regulation of DNA damage response in DOX-treated cells [44]. DOX induces the phosphorylation of histone H2AX on Ser^{139} (γH2AX) and DNA damage foci formation [45-47].

To examine the effects of diarylheptanoids on double strand DNA breaks, HaCaT cells were incubated for 18 h with 5 μM **1, 2** or CUR and 20 nM DOX in single and combination treatments. Single treatments with **1, 2** or CUR did not cause a significant amount of double strand DNA breaks in HaCaT cells nuclei compared to DOX damaging

activity (Fig. 3A). Pretreatments with **1** and **2** resulted in a major reduction of genomic DNA damage induced by a single DOX treatment. Co-incubation with CUR did not alter the effect of DOX (Fig. 3A). Double strand DNA breaks labeled with anti-phospho-histone H2A.X antibody were quantified by flow cytometry analysis. DOX treatment in HaCaT cells pretreated with diarylheptanoids **1** and **2** did not generate prominent DNA damage observed after single treatment with doxorubicin (Fig. 3B). Moreover, single treatment with compound **2** further reduced the amount of double strand DNA breaks found in untreated cells (Fig. 3B). While single treatment with CUR also decreased DNA breakage compared to untreated cells, it did not manage to overcome the damaging effect of DOX. Quantification and statistical analysis of phosphorylated histone H2AX detected by flow cytometry is presented in Fig. 3C. We previously reported that **1** and **2** cause the retention of DOX in the cytoplasm of HaCaT cells [23]. In order to reach its target molecules, DNA and topoisomerase II, DOX needs to enter the nucleus, therefore this finding may contribute the mechanisms behind DNA protection by diarylheptanoids.

Although diarylheptanoids **1** and **2** display multiple DOX-protective effects *in vitro*, the presence of glycosidic moiety could potentially interfere with their absorption *in vivo*. Nevertheless, there are various methods to amplify the bioavailability, ensure longer circulation, better permeability, and resistance to metabolic processes of orally or topically administered compounds [48]. Application of nanoparticles, liposomal, cyclodextrin or polylactic-co-glycolic acid encapsulation, and co-administation with other agents could all potentially improve systematic delivery of drugs such as curcumin [48]. Undoubtedly, further experiments are needed to address DOX-protective actions of investigated diarylheptanoids in *in vivo* model systems.

*Diarylheptanoids **1** and **2** promote wound healing and rearrange F-actin in human normal keratinocytes*

Human skin consists of various cell types including keratinocytes, melanocytes, and fibroblasts [49]. HaCaT are human immortalized keratinocyte cells, which play an essential role in epidermal tissue regeneration. This cell line underwent a spontaneous transformation to cells which possess the characteristics of basal epidermal keratinocytes, and can be delivered in deep burns. For this reason, HaCaT cell line represents a very useful model for highly proliferative epidermis in pathological skin conditions and has been included in multiple wound healing, transplantation, and cell culture studies [50-54].

In this investigation, we used wound healing assay to address the influence of **1**, **2** and CUR on HaCaT cell migration. HaCaT cells were treated with 5 μM **1** or **2** and cell migration was compared to 5 μM CUR treatment after 24 h (Fig. 4A). While CUR showed no significant effect on cell motility, compounds **1** and **2** promoted wound healing in HaCaT cells (Fig. 4B). Other authors findings regarding CUR migration effects were contradictory: negative impact on migration was shown in lung cancer cells [55-56], while stimulation of proliferation and migration was detected in olfactory unsheathing cells [57].

Next, we followed whether the changes in cell motility after diarylheptanoids treatment could be accompanied by the formation of podosomes and lamellipodia in HaCaT cells. For that purpose, we labeled HaCaT cells with ActinRed™ 555 and visualized the actin cytoskeleton under the fluorescent microscope after treatments with 5 μM of **1**, **2** and CUR for 24 h (Fig. 4C). Our results showed that compounds **1** and **2**

promoted podosome and lamellipodia formation besides cell migration and wound healing in HaCaT cells. Although 5 μM CUR did not significantly influence cell motility after 24 h, it exhibited a prominent effect on actin morphology in HaCaT cells, similarly to diarylheptanoids **1** and **2** (Fig. 4C).

Conclusion

In the search for anti-cancer agents from natural sources, two types of beneficial compounds may be identified: the ones with the capacity to inhibit the cancer cell growth and the others with protective properties in normal cells during the course of chemotherapy. Anti-cancer agents such as DOX induce DNA breakage, reactive oxygen species (ROS) formation, and apoptosis in both cancer and non-cancerous dividing cells. We found that diarylheptanoids isolated from the bark of black alder (*Alnus glutinosa*) may provide protection to normal cells reducing their sensitivity to the damage generated by DOX application. Considering the observed effect on the keratinocyte motility, the application of diarylheptanoids could be a promising approach for further dermo-protection and skin regeneration studies. However, additional research is required to establish diarylheptanoids, particularly compound **2**, as protective agents for non-cancerous dividing cells during chemotherapy of cancer patients.

Acknowledgements

This research was supported by Ministry of Education, Science and Technological Development of Serbia (grant no. III 41031).

Conflict of interest

The authors declare no conflict of interest.

Figure legends

Fig. 1. Diarylheptanoids **1** and **2** desensitize HaCaT cells to DOX.

(**A**) Chemical structures of diarylheptanoids **1**, **2** and CUR. (**B**) IC_{50} values for DOX after pretreatment with 5 μM diarylheptanoids **1**, **2** and CUR in HaCaT cells. (**C**) The effects of subsequent combinations of 5 μM diarylheptanoids **1**, **2** or CUR with DOX in HaCaT cells. The effects were assessed by MTT assay after 72 h. The nature of interactions between compounds was analyzed by CalcuSyn software and presented as log10 (CI) values. All combinations of **1** and **2** with DOX exhibited antagonistic effect (log10 (CI) > 0).

Fig. 2. Diarylheptanoid **2** prevents cell death induced by DOX in HaCaT cells by promoting autophagy.

(**A**) Cell death induction by 5 μM **1** or **2** in single and combined treatments with 40 nM DOX in HaCaT cells. The samples were analyzed for green fluorescence (Annexin-V-FITC, FL1-H) and red fluorescence (Propidium Iodide, FL2-H) by flow-cytometry. (**B**) Quantification and statistical analysis of flow-cytometric cell death measurements in HaCaT cells. Statistical analysis was performed by two-way ANOVA test. Statistical significance between untreated and treated samples is presented as $p<0.01$ (**) and $p<0.05$ (*). Statistical significance between DOX treatment and combination treatments is presented as $p<0.05$ (#). (**C**) Induction of autophagy in HaCaT cells. Accumulation of autophagosomes (green) in the cytoplasm after treatments with 5 μM of **1, 2** and CUR

was visualized by anti-LC3B antibody staining. HaCaT cells were treated with 250 nM mTOR inhibitor AZD2014, an autophagy-inducing agent as a positive control. Scale bar = 100 μm. (**D**) Flow-cytometric profiles of HaCaT cells treated with with 5 μM of **1, 2** and CUR or 250 nM AZD2014 and labeled with anti-LC3B antibody to detect autophagic flux. (**E**) Quantification and statistical analysis of flow-cytometric autophagic flux measurements in HaCaT cells. Statistical significance was determined by one-way ANOVA test and is presented as $p<0.001$ (***) and $p<0.01$ (**).

Fig. 3. Diarylheptanoids protect HaCaT cells against DOX-induced DNA damage. (**A**) 5 μM diarylheptanoids **1**, **2** and CUR were applied in single and combined treatments with 20 nM DOX. Double strand DNA breaks were labeled with phospho-histone H2A.X antibody (red). Nuclei were counterstained with Hoechst 33342 (blue). Scale bar = 100 μm. (**B**) Flow-cytometric profiles of HaCaT cells after single diarylheptanoid treatments and combined treatments with DOX. Cells were labeled with anti-phospho-histone H2A.X antibody to detect double strand DNA breaks. (**C**) Quantification and statistical analysis of flow-cytometric measurements of double strand DNA breaks in HaCaT cells. Statistical analysis was performed by one-way ANOVA test. Statistical significance between untreated and treated samples is presented as $p<0.001$ (***), $p<0.01$ (**) and $p<0.05$ (*). Statistical significance between DOX treatment and combination treatments is presented as $p<0.001$ (###), $p<0.01$ (##).

Fig. 4. Diarylheptanoids promote wound healing and rearrange F-actin in HaCaT cells.

(**A**) The effect of 24 h treatment with 5 μM **1**, **2** and CUR on wound healing in HaCaT cells. (**B**) Measurement of HaCaT cell migration. The *y*-axis represents relative wound closure compared to untreated sample. Statistical significance between treated and

untreated cells was determined by Student's t-test and is presented as $p<0.001$ (***) and $p<0.05$ (*). (**C**) Treatment with 5 μM **1**, **2** and CUR for 24 h causes formation of podosomes and lamellipodia in HaCaT cells. F-actin was visualized by ActinRed™ 555 staining (green). Nuclei were counterstained with Hoechst 33342 (blue). Scale bar = 100 μm.

References

[1] Farnsworth, N.R., Soejarto, D.D., Potential consequences of plant extinction in the United States on the current and future availability of prescription drugs., Econ Bot. 3 (1985) 231-40.
[2] Cordell, G.A., Recent developments in the study of biologically active natural products, ACGC Chem Commun. (2002) 31–63.
[3] Sati, S.C., Sati, N., Sati, O.P., Bioactive constituents and medicinal importance of genus Alnus, Pharmacogn Rev. 5 (2011) 174-83.
[4] O'Rourke, C., Byres, M., Delazar, A., Kumarasamy, Y., Nahar, L., Stewart, F., et al., Hirsutanonol, oregonin and genkwanin from the seeds of Alnus glutinosa (Betulaceae). Biochem Syst Ecol. (2005) 749–52.
[5] Kumarasamy, Y., Cox, P.J., Jaspars, M., Nahar, L., Sarker, S.D., Bioactivity of hirsutanolol, oregonin and genkwanin, isolated from the seeds of Alnus glutinosa (Betulaceae). Nat Prod Commun. (2006) 641–4.
[6] Novakovic, M., Stankovic, M., Vuckovic, I., Todorovic, N., Trifunovic, S., Tesevic, V., et al., Diarylheptanoids from Alnus glutinosa bark and their chemoprotective effect on human lymphocytes DNA, Planta Med. 79 (2013) 499-505.
[7] Novakovic, M., Pesic, M., Trifunovic, S., Vuckovic, I., Todorovic, N., Podolski-Renic, A., et al., Diarylheptanoids from the bark of black alder inhibit the growth of sensitive and multi-drug resistant non-small cell lung carcinoma cells, Phytochemistry. 97 (2014) 46-54.
[8] Brand, S., Holscher, D., Schierhorn, A., Svatos, A., Schroder, J., Schneider, B., A type III polyketide synthase from Wachendorfia thyrsiflora and its role in diarylheptanoid and phenylphenalenone biosynthesis, Planta. 224 (2006) 413-28.
[9] Munde, T., Brand, S., Hidalgo, W., Maddula, R.K., Svatos, A., Schneider, B., Biosynthesis of tetraoxygenated phenylphenalenones in Wachendorfia thyrsiflora, Phytochemistry. 91 (2013) 165-76.
[10] Aggarwal, B.B., Harikumar, K.B., Potential therapeutic effects of curcumin, the anti-inflammatory agent, against neurodegenerative, cardiovascular, pulmonary, metabolic, autoimmune and neoplastic diseases, Int J Biochem Cell Biol. 41 (2009) 40-59.

[11] Gupta, S.C., Patchva, S., Koh, W., Aggarwal, B.B., Discovery of curcumin, a component of golden spice, and its miraculous biological activities, Clin Exp Pharmacol Physiol. 39 (2012) 283-99.
[12] Baliga, M.S., Joseph, N., Venkataranganna, M.V., Saxena, A., Ponemone, V., Fayad, R., Curcumin, an active component of turmeric in the prevention and treatment of ulcerative colitis: preclinical and clinical observations, Food Funct. 3 (2012) 1109-17.
[13] Chidambara Murthy, K.N., Jayaprakasha, G.K., Patil, B.S., Citrus limonoids and curcumin additively inhibit human colon cancer cells, Food Funct. 4 (2013) 803-10.
[14] Nazari, Q.A., Takada-Takatori, Y., Hashimoto, T., Imaizumi, A., Izumi, Y., Akaike, A., et al., Potential protective effect of highly bioavailable curcumin on an oxidative stress model induced by microinjection of sodium nitroprusside in mice brain, Food Funct. 5 (2014) 984-9.
[15] Matsuda, H., Ishikado, A., Nishida, N., Ninomiya, K., Fujiwara, H., Kobayashi, Y., et al., Hepatoprotective, superoxide scavenging, and antioxidative activities of aromatic constituents from the bark of Betula platyphylla var. japonica, Bioorg Med Chem Lett. 8 (1998) 2939-44.
[16] Tung, N.H., Kim, S.K., Ra, J.C., Zhao, Y.Z., Sohn, D.H., Kim, Y.H., Antioxidative and hepatoprotective diarylheptanoids from the bark of Alnus japonica, Planta Med. 76 (2010) 626-9.
[17] Lai, Y.C., Chen, C.K., Lin, W.W., Lee, S.S., A comprehensive investigation of anti-inflammatory diarylheptanoids from the leaves of Alnus formosana, Phytochemistry. 73 (2012) 84-94.
[18] Tung, N.H., Kwon, H.J., Kim, J.H., Ra, J.C., Ding, Y., Kim, J.A., et al., Anti-influenza diarylheptanoids from the bark of Alnus japonica, Bioorg Med Chem Lett. 20 (2010) 1000-3.
[19] Choi, S.E., Kim, K.H., Kwon, J.H., Kim, S.B., Kim, H.W., Lee, M.W., Cytotoxic activities of diarylheptanoids from Alnus japonica, Arch Pharm Res. 31 (2008) 1287-9.
[20] Liu, J.X., Di, D.L., Wei, X.N., Han, Y., Cytotoxic diarylheptanoids from the pericarps of walnuts (Juglans regia), Planta Med. 74 (2008) 754-9.
[21] Sun, Y., Tabata, K., Matsubara, H., Kitanaka, S., Suzuki, T., Yasukawa, K., New cytotoxic diarylheptanoids from the rhizomes of Alpinia officinarum, Planta Med. 74 (2008) 427-31.
[22] Mshvildadze, V., Legault, J., Lavoie, S., Gauthier, C., Pichette, A., Anticancer diarylheptanoid glycosides from the inner bark of Betula papyrifera, Phytochemistry. 68 (2007) 2531-6.
[23] Dinic, J., Novakovic, M., Podolski-Renic, A., Stojkovic, S., Mandic, B., Tesevic, V., et al., Antioxidative activity of diarylheptanoids from the bark of black alder (Alnus glutinosa) and their interaction with anticancer drugs, Planta Med. 80 (2014) 1088-96.
[24] Chou, T.C., Talalay, P., Quantitative analysis of dose-effect relationships: the combined effects of multiple drugs or enzyme inhibitors, Adv Enzyme Regul. 22 (1984) 27-55.
[25] Mizutani, H., Tada-Oikawa, S., Hiraku, Y., Kojima, M., Kawanishi, S., Mechanism of apoptosis induced by doxorubicin through the generation of hydrogen peroxide, Life Sci. 76 (2005) 1439-53.
[26] Wang, S., Konorev, E.A., Kotamraju, S., Joseph, J., Kalivendi, S., Kalyanaraman, B., Doxorubicin induces apoptosis in normal and tumor cells via distinctly different

mechanisms. intermediacy of H(2)O(2)- and p53-dependent pathways, J Biol Chem. 279 (2004) 25535-43.
[27] Eom, Y.W., Kim, M.A., Park, S.S., Goo, M.J., Kwon, H.J., Sohn, S., et al., Two distinct modes of cell death induced by doxorubicin: apoptosis and cell death through mitotic catastrophe accompanied by senescence-like phenotype, Oncogene. 24 (2005) 4765-77.
[28] Eskelinen, E.L., Saftig, P., Autophagy: a lysosomal degradation pathway with a central role in health and disease, Biochim Biophys Acta. 1793 (2009) 664-73.
[29] Aredia, F., Scovassi, A.I., Manipulation of autophagy in cancer cells: an innovative strategy to fight drug resistance, Future Med Chem. 5 (2013) 1009-21.
[30] Kumar, P., Zhang, D.M., Degenhardt, K., Chen, Z.S., Autophagy and transporter-based multi-drug resistance, Cells. 1 (2012) 558-75.
[31] Marino, G., Niso-Santano, M., Baehrecke, E.H., Kroemer, G., Self-consumption: the interplay of autophagy and apoptosis, Nat Rev Mol Cell Biol. 15 (2014) 81-94.
[32] Yang, Z., Klionsky, D.J., Mammalian autophagy: core molecular machinery and signaling regulation, Curr Opin Cell Biol. 22 (2010) 124-31.
[33] Nakatogawa, H., Two ubiquitin-like conjugation systems that mediate membrane formation during autophagy, Essays Biochem. 55 (2013) 39-50.
[34] Kabeya, Y., Mizushima, N., Yamamoto, A., Oshitani-Okamoto, S., Ohsumi, Y., Yoshimori, T., LC3, GABARAP and GATE16 localize to autophagosomal membrane depending on form-II formation, J Cell Sci. 117 (2004) 2805-12.
[35] Warnes, G., Measurement of autophagy by flow cytometry, Curr Protoc Cytom. 68 (2014) 9 45 1-9 10.
[36] Shvets, E., Elazar, Z., Flow cytometric analysis of autophagy in living mammalian cells, Methods Enzymol. 452 (2009) 131-41.
[37] Hundeshagen, P., Hamacher-Brady, A., Eils, R., Brady, N.R., Concurrent detection of autolysosome formation and lysosomal degradation by flow cytometry in a high-content screen for inducers of autophagy, BMC Biol. 9 (2011) 38.
[38] Cao, J., Liu, Y., Jia, L., Zhou, H.M., Kong, Y., Yang, G., et al., Curcumin induces apoptosis through mitochondrial hyperpolarization and mtDNA damage in human hepatoma G2 cells, Free Radic Biol Med. 43 (2007) 968-75.
[39] Roy, M., Sinha, D., Mukherjee, S., Biswas, J., Curcumin prevents DNA damage and enhances the repair potential in a chronically arsenic-exposed human population in West Bengal, India, Eur J Cancer Prev. 20 (2011) 123-31.
[40] Srinivasan, M., Rajendra Prasad, N., Menon, V.P., Protective effect of curcumin on gamma-radiation induced DNA damage and lipid peroxidation in cultured human lymphocytes, Mutat Res. 611 (2006) 96-103.
[41] Cao, J., Jia, L., Zhou, H.M., Liu, Y., Zhong, L.F., Mitochondrial and nuclear DNA damage induced by curcumin in human hepatoma G2 cells, Toxicol Sci. 91 (2006) 476-83.
[42] Fornari, F.A., Randolph, J.K., Yalowich, J.C., Ritke, M.K., Gewirtz, D.A., Interference by doxorubicin with DNA unwinding in MCF-7 breast tumor cells, Mol Pharmacol. 45 (1994) 649-56.
[43] Pommier, Y., Leo, E., Zhang, H., Marchand, C., DNA topoisomerases and their poisoning by anticancer and antibacterial drugs, Chem Biol. 17 (2010) 421-33.

[44] Pang, B., Qiao, X., Janssen, L., Velds, A., Groothuis, T., Kerkhoven, R., et al., Drug-induced histone eviction from open chromatin contributes to the chemotherapeutic effects of doxorubicin, Nat Commun. 4 (2013) 1908.
[45] Jaamaa, S., Af Hallstrom, T.M., Sankila, A., Rantanen, V., Koistinen, H., Stenman, U.H., et al., DNA damage recognition via activated ATM and p53 pathway in nonproliferating human prostate tissue, Cancer Res. 70 (2010) 8630-41.
[46] Zhou, F., Mei, H., Wu, Q., Jin, R., Expression of histone H2AX phosphorylation and its potential to modulate adriamycin resistance in K562/A02 cell line, J Huazhong Univ Sci Technolog Med Sci. 31 (2011) 154-8.
[47] Kurz, E.U., Douglas, P., Lees-Miller, S.P., Doxorubicin activates ATM-dependent phosphorylation of multiple downstream targets in part through the generation of reactive oxygen species, J Biol Chem. 279 (2004) 53272-81.
[48] Prasad, S., Tyagi, A.K., Aggarwal, B.B., Recent developments in delivery, bioavailability, absorption and metabolism of curcumin: the golden pigment from golden spice, Cancer Res Treat. 46 (2014) 2-18.
[49] Ji, Y., Li, X.T., Chen, G.Q., Interactions between a poly(3-hydroxybutyrate-co-3-hydroxyvalerate-co-3-hydroxyhexanoate) terpolyester and human keratinocytes, Biomaterials. 29 (2008) 3807-14.
[50] Garcia, J.L., Asadinezhad, A., Pachernik, J., Lehocky, M., Junkar, I., Humpolicek, P., et al., Cell proliferation of HaCaT keratinocytes on collagen films modified by argon plasma treatment, Molecules. 15 (2010) 2845-56.
[51] Lehmann, B., HaCaT cell line as a model system for vitamin D3 metabolism in human skin, J Invest Dermatol. 108 (1997) 78-82.
[52] Boelsma, E., Verhoeven, M.C., Ponec, M., Reconstruction of a human skin equivalent using a spontaneously transformed keratinocyte cell line (HaCaT), J Invest Dermatol. 112 (1999) 489-98.
[53] Maas-Szabowski, N., Starker, A., Fusenig, N.E., Epidermal tissue regeneration and stromal interaction in HaCaT cells is initiated by TGF-alpha, J Cell Sci. 116 (2003) 2937-48.
[54] Meineke, V., Muller, K., Ridi, R., Cordes, N., Kohn, F.M., Mayerhofer, A., et al., Development and evaluation of a skin organ model for the analysis of radiation effects, Strahlenther Onkol. 180 (2004) 102-8.
[55] Chen, Q.Y., Zheng, Y., Jiao, D.M., Chen, F.Y., Hu, H.Z., Wu, Y.Q., et al., Curcumin inhibits lung cancer cell migration and invasion through Rac1-dependent signaling pathway, J Nutr Biochem. 25 (2014) 177-85.
[56] Lin, S.S., Lai, K.C., Hsu, S.C., Yang, J.S., Kuo, C.L., Lin, J.P., et al., Curcumin inhibits the migration and invasion of human A549 lung cancer cells through the inhibition of matrix metalloproteinase-2 and -9 and Vascular Endothelial Growth Factor (VEGF), Cancer Lett. 285 (2009) 127-33.
[57] Tello Velasquez, J., Watts, M.E., Todorovic, M., Nazareth, L., Pastrana, E., Diaz-Nido, J., et al., Low-dose curcumin stimulates proliferation, migration and phagocytic activity of olfactory ensheathing cells, PLoS One. 9 (2014) e111787.

Table 1. Cell growth inhibitory effects of diarylheptanoids **1**, **2**, CUR, and a classic chemotherapeutic agent DOX in normal human keratinocytes (HaCaT) and melanoma cells (518A2). Data shown are means ± s. e. m. Statistical significance was determined by two-way ANOVA test and is presented as $p<0.001$ (***) and $p<0.01$ (**).

Drugs	**IC_{50}** (μM)	
	HaCaT	**518A2**
1	9.2 ± 1.15	15.78 ± 1.31 ***
2	35.17 ± 1.22	24 ± 1.19 **
CUR	7.44 ± 1.15	48.32 ± 1.39 ***
DOX	0.0067 ± 0.00127	0.0245 ± 0.00125 ***

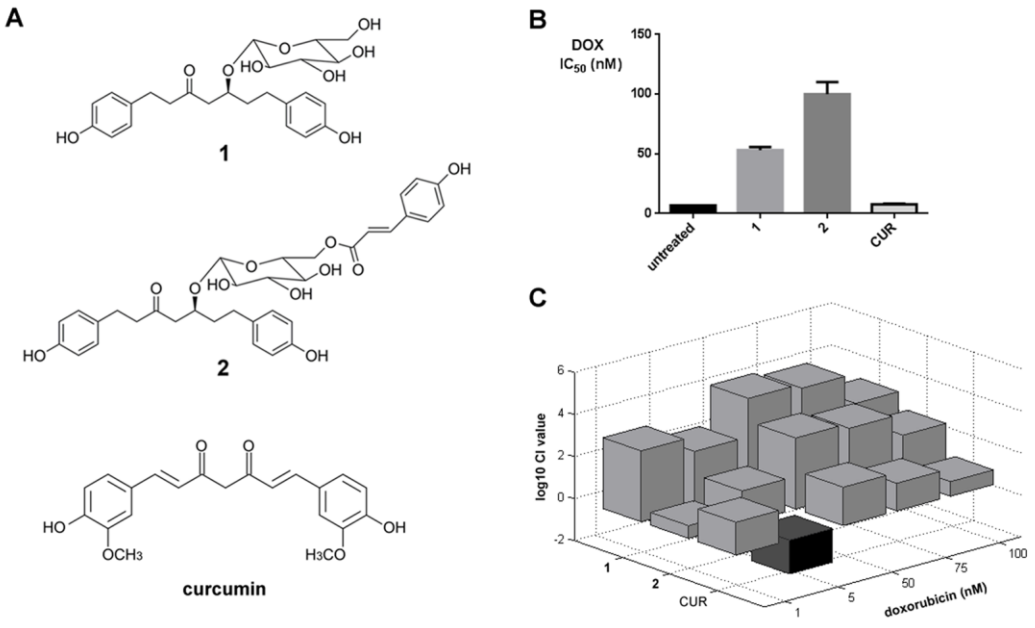

Fig. 1

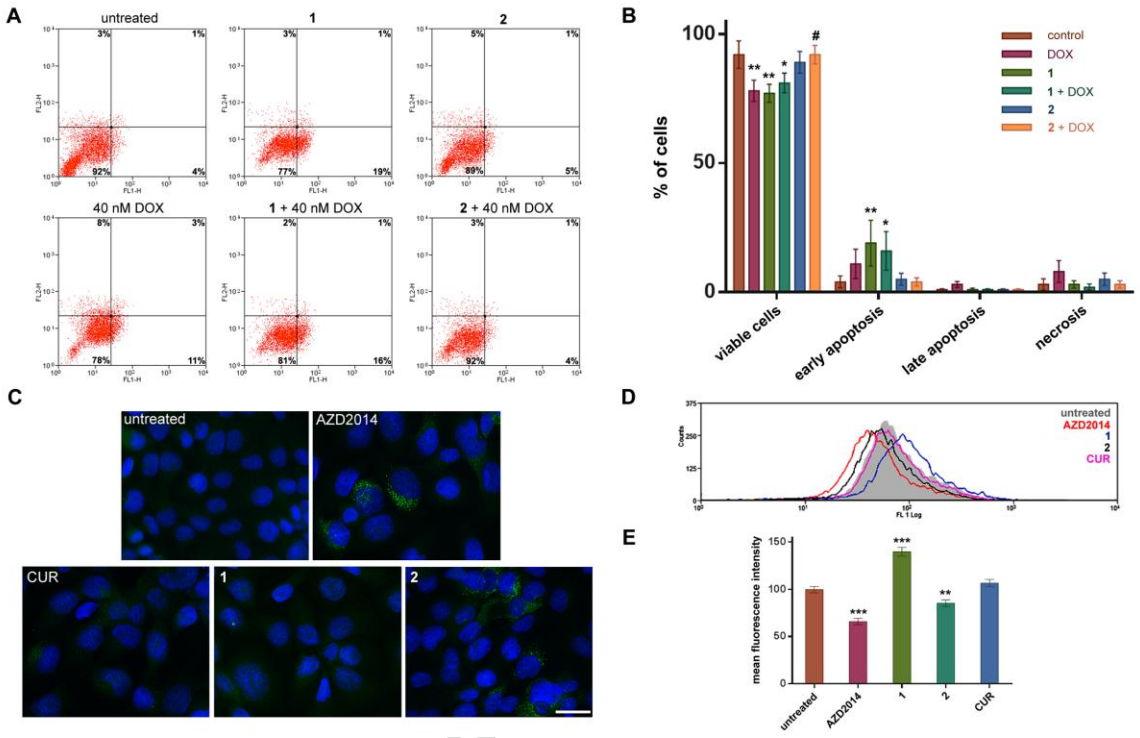

Fig. 2

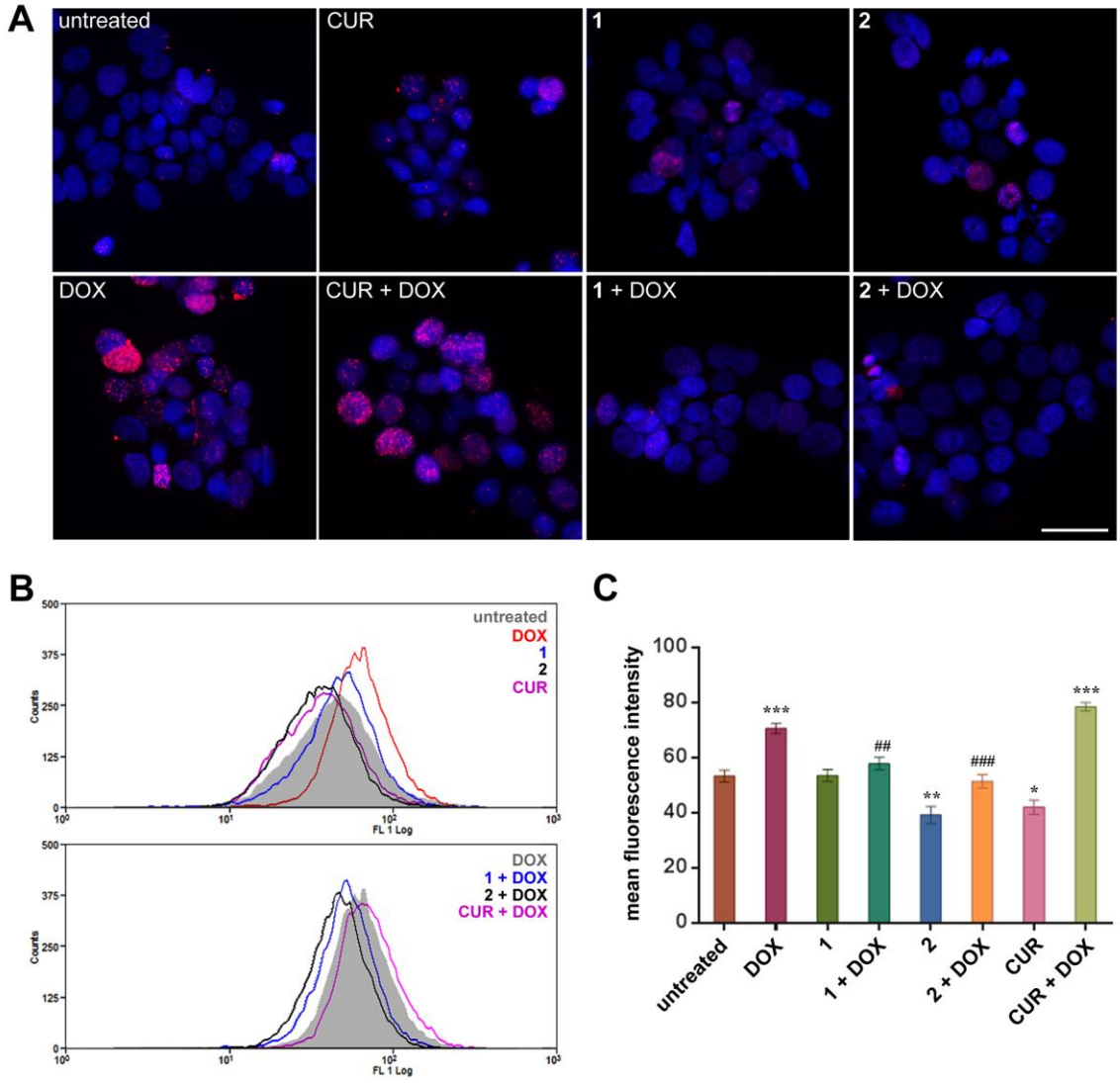

Fig. 3

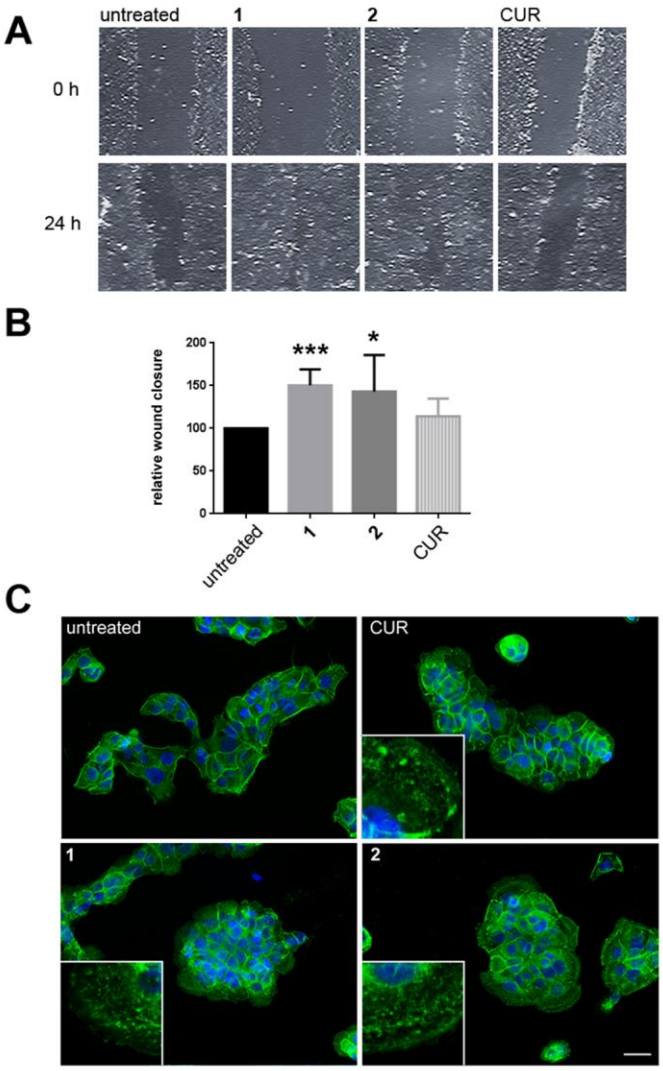

Fig. 4

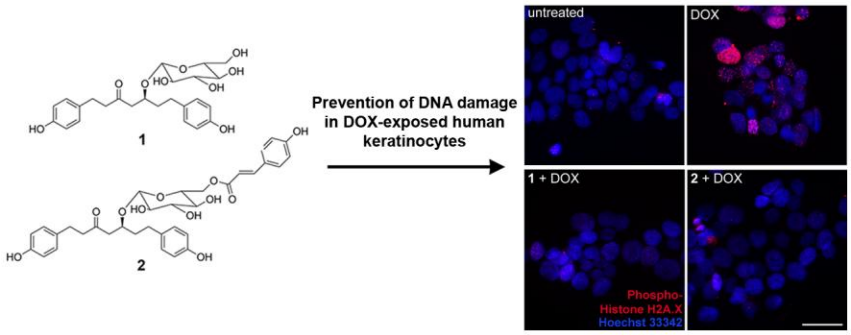

Graphical Abstract